OPEN ACCESS

University of BRISTOL

Peer reviewed version

Link to published version (if available):
10.2514/6.2017-0630

Link to publication record in Explore Bristol Research
PDF-document

University of Bristol - Explore Bristol Research
General rights

Testing of Wing-Tip Spring Device for Gust Loads Alleviation

R.C.M. Cheung[1], A. Castrichini[2], D. Rezgui[3], J.E. Cooper[4]
University of Bristol, Department of Aerospace Engineering, University Walk, Bristol, BS8 1TR, UK.

and

T. Wilson[5]
Airbus Operations Ltd, Filton, Bristol, BS34 7PA, UK.

Recent aircraft designs have begun considering higher aspect ratio wings to reduce induced drag for improved fuel efficiency. In order to meet airport gate requirements, folding wing-tips have been introduced as a solution to the increased wing-span. Recent numerical studies have suggested such a folding wing-tip solution may be incorporated with spring devices in order to provide an additional gust loads alleviation ability in flight. A series of low-speed wind tunnel tests was conducted using a prototype of such a concept and found that a folding wing-tip with a non-zero relative angle of the folding hinge axis to the stream-wise direction can provide gust loads alleviation. It was also concluded that the weight of the wing-tip may have a strong influence on the hinge stiffness necessary for best performance. The findings from these tests agree with previous simulations in a qualitative manner.

Nomenclature

α	=	Angle of attack
Λ	=	Sweep angle
θ	=	Fold angle of the wing-tip
γ	=	Hinge angle
k_θ	=	Torsional spring stiffness
k_x	=	Linear spring stiffness
V	=	Wind tunnel speed

I. Introduction

FROM the classic Breguet range equation, aircraft with more fuel-efficient engines, lower aerodynamic drag or lower structural weight can fly further. Therefore, an aircraft with any of these attributes can cover the same distance carrying higher payload or using less fuel as well. For airframe design, this means targeting the aerodynamics and structural weight. One approach for improving the aerodynamics is through increasing the aspect ratio of the wing, which decreases the associated induced drag. However, increasing the wing span not only increases structural weight, it could also lead to operating difficulties as existing airport gates may be too narrow. Trying to achieve these two contrasting planform requirements in fact points towards the wider field of morphing structure research, which focuses on changing the geometry of the aircraft during its operation. The field of morphing covers larger geometric[1,] changes including sweep and span to finer shape changes such as camber and section thickness, which tend to be more focused on application of specific materials[2-4, 6] or fabricated products[7].

One of the simplest morphing solutions for variable span requirement is in the form of a folding wing-tip, which is already deployed in the latest civil airlines[8], as it can be achieved using conventional materials through a hinged design. The hinge mechanism allows the wing-tip to be folded up as the aircraft taxis to the gate and locked in its extended position before takeoff. Morphing of the wing-tip has in fact received significant interest within the field itself as the wing-tip has been identified with great potentials to fulfil a wider goal of enabling optimized performance in varying conditions throughout the flight. The main benefit of wing-tip morphing is its relatively small size compared to the planform, yet it can have a large influence on wing root loading due to its considerable distance from the wing root itself as well as being aerodynamically important for stall, drag and maneuverability.

For gust loads alleviation, the large moment arm offered by the wing-tip for influencing the wing root bending moment has been the main reason for their selection in their respective studies, which include Miller[9-10], Guo[11-12] and Ricci[13] who considered a passive movable aerodynamic surface at the wing-tip. The device was connected to the main airframe through a torque tube in the span-wise direction, which provided additional torsional stiffness about a location forward of the wing-tip's center of pressure. The device functioned by reacting to vertical gusts through nose-down deflection in a passive manner, which alleviated the load increment caused by the gusts in the process. Although good loads alleviation capability was observed, it had a detrimental effect on flutter, especially when low torsional stiffness torque tubes were used.

Another approach for gust loads alleviation is through a folding wing-tip device that has an offset hinge axis from the longitudinal axis of the aircraft. The idea for such a device originates from the observation that when the orientation of the axis of which folding of the wing-tip occurs is strongly linked to the effective geometric twist of the wing-tip as it folds, which is described by

$$\Delta\alpha = -\tan^{-1}(\tan\theta \sin\gamma) \tag{1}$$

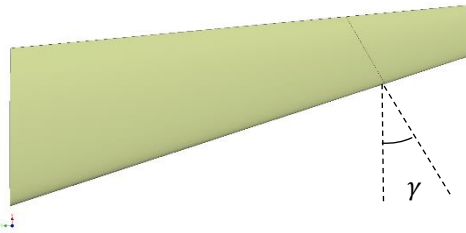where the orientation of the axis is expressed as a function of the hinge angle γ in Figure 1 and the fold angle θ in Figure 2.

Figure 1. Planform view showing the hinge angle γ.

Figure 2. Front view showing the fold angle θ.

Hence, the zero-value hinge angle shown in Figure 3 provides no gust loads alleviation capability, whereas a positive hinge angle, as shown in Figure 4, could provide potential loads alleviation benefit during vertical gust encounters due to the decreased twist (local angle of attack) beyond the fold, as this action reduces the resulting bending moment contribution.

Figure 3. Front view showing positive fold angle for a hinge angle of 0^0.

Figure 4. Front view showing positive fold angle for a hinge angle of 30^0.

American Institute of Aeronautics and Astronautics

Therefore, a folding wing-tip has the potential to fulfil both the airport gate requirement and to provide gust loads alleviation capability by incorporating a non-zero hinge angle in its design. In fact, a number of numerical studies have been carried out to investigate the feasibility and performance of using a device of this type, in addition to a passive spring system at the hinge in order to control its dynamic behavior and exploit its potential gust loads alleviation capability. A preliminary study[14] has found that a linear spring device can provide load-alleviating benefit when both the hinge stiffness and wing-tip inertia are low. However, low hinge stiffness can cause the wing-tip to remain in a deflected position even in a trimmed-flight condition, which has an undesirable effect on the overall aerodynamics. This differing optimal stiffness for trimmed-flight and gust loads alleviation has led to proposed solutions such as bi-stable wing-tips[15] and active control via piezoelectric actuators[16]. Despite this complication, the folding wing-tip concept remains promising as recent research have suggested that coupling the folding wing-tip to a nonlinear spring system may provide the solution[17, 18].

The work described in this paper aims to obtain baseline experimental data of the folding wing-tip concept when coupled with a linear spring device, particularly focusing on the effect of a non-zero hinge angle has on the its gust loads alleviation performance through low-speed wind tunnel testing.

II. Wind Tunnel Model

A. Design

One of the aims of this investigation is to establish the effect of a non-zero hinge angle has on the overall gust loads alleviation performance. Since the primary measure of gust loads alleviation is the reduction in peak wing root bending moment, the wind tunnel model design has been maximized to the largest permissible semi-span for the wind tunnel working section at approximately 0.7m with a constant un-swept chord of 0.3m, using a symmetric NACA0015 section profile.
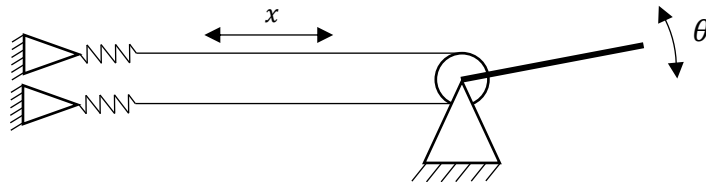

**Figure 5. Schematic of the spring system**

Despite using a comparatively thick NACA0015 section, the internal height remains restrictive for fitting a spring system. Therefore, a cable linkage has been devised to connect the folding wing-tip to a spring system situated outside the wind tunnel. The cable linkage translates angular displacement of the wing-tip into a translational displacement of the cable, as shown in Figure 5, which enables the use of linear tension springs to represent a torsional spring fitted at the hinge. The equivalent torsional stiffness is given by

$$k_\theta = k_x \frac{dx}{d\theta} \tag{2}$$

As shown in Figure 6, the fixture at the hinge has been designed so that the cables will always depart at the same direction and distance away from the hinge, thus ensuring the derivative in Equation (2) is constant and a linear mapping is retained. The dual cable design enables both cables to remain in tension at all fold angles through pre-tensioning, thus ensuring consistency in the spring tension provided by both springs.
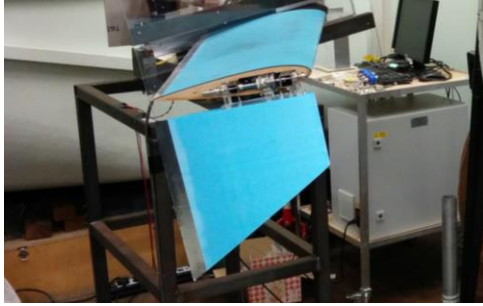
(a) The folding wing-tip
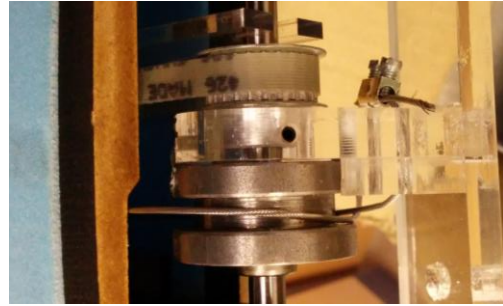
(b) Cable fixture at the folding hinge

Figure 6. Wind tunnel model

With future testing in mind, a decision has been made to incorporate variable sweep into the wind tunnel model, while keeping the hinge axis fixed relative to the body of the model itself. This approach allows the effective hinge angle to be varied through a change in sweep angle, as well as keeping swapping of parts to a minimum. The orientation of the hinge axis is normal to the leading edge, which gives a simple mapping between the hinge angle and the sweep angle.

$$\gamma = \Lambda \tag{3}$$

As illustrated in Figure 7, the variable sweep design requires shielding the trailing edge region at the wing root from the flow as the sweep angle is increased, which has a secondary effect in changing the total exposed wing area and span. To compensate for these changes, a customized wing-tip is used at each sweep angle to be tested. Each wing-tip is sized to approximately 25% of the total exposed wing area of its corresponding test configuration, and shaped such that the tip of the overall wing terminates in a consistent manner. Foam construction has been chosen to ease the manufacturing process, as well as minimizing the inertia and mass of the wing-tips. For the experimental work presented in this paper, only one the sweep angle setting was used, which was at 30°.

(a) Low sweep angle

(b) High sweep angle

Figure 7. Variable sweep design

B. Test set-up and instrumentation

The wind tunnel tests were conducted in the open-jet wind tunnel at the University of Bristol, as shown in Figure 8(a). The test campaign consisted of a set of steady aerodynamic tests and a set of dynamic tests in the form of gust excitation. The sweep angle of the wind tunnel model was kept at 30°, which corresponds to a hinge angle of 30°. The measurements recorded in each test case were lift, rolling moment, fold angle and hinge moment at the folding hinge. For assessing gust loads alleviation performance, the rolling moment is the key measurement since it can be translated directly to the wing root bending moment that the aircraft may experience. The main body forces and moments were measured using a custom-built frame in combination of two AMTI MC3A force and torque sensors[19], while the fold angle was monitored using a RLS RE22 rotary magnetic shaft encoder[20]. The hinge moment was derived from the cable tension measured through two RDP Model 31 load cells[21]. Data acquisition was enabled using a National Instruments USB-6211 and LabVIEW software[22].

For the steady aerodynamic tests, a stiff-hinge and a free-hinge configuration were used, while the dynamic test included both in addition to a sprung-hinge configuration. The sprung-hinge configuration was set up as illustrated in Figure 5, using two linear springs, each with measured stiffness of 195N/m. This set-up gave an equivalent torsional stiffness of 0.043Nm/rad as the pulley radius was 10.5mm. The pre-load applied to these springs were such that the net hinge moment due to the springs was near zero at fold angle of 0°. The stiff-hinge configuration was achieved by removing the springs and connecting the cables directly to the load cells, while the free-hinge configuration was set up simply through disconnecting the cables from the wing-tip.

The dynamic tests additionally involved installing a gust vane, as pictured in Figure 8(b), ahead of the wind tunnel model to perturb the oncoming flow. The gust vane was actuated manually through a mass-spring system, whereby a consistent initial displacement of the counter-weight produced a consistent excitation to the flow field through deflection of the gust vane. At each test point, an upward and a downward perturbation were performed, each initiated through displacement of the counter-weight by a predetermined distance in the appropriate direction.

(a) Steady aerodynamic test   (b) Gust excitation test

**Figure 8. Wind tunnel test set-up**

III.   Results

The wind tunnel model was tested at its 30° hinge angle configuration, corresponding to a sweep angle of 30°, with reference semi-span of 0.695m and reference chord length of 0.346m.

A. Steady aerodynamics

In this test, the stiff-hinge and free-hinge configuration were examined; with angle of attack varying from -10° to 10° in increments of 5° and wind speed at 10, 12, 15, 18 and 20m/s. At every test point, the wing-tip settled to a steady fold angle once the flow had stabilized, demonstrating a degree of aerodynamic stability as expected.

Figure 9 shows that the lift-curve of the stiff-hinge configuration was linear, akin to a non-folding configuration, while variation of the lift-curve slope was observed in the free-hinge configuration at different wind speeds. It appears that at lower speeds, the free-hinge configuration generated larger amount of lift, which is consistent with the negative fold angles as shown in Figure 11. This larger total lift is the result of the additional nose-up twist of the wing-tip caused by the negative fold angle. As shown in Figure 10, this additional lift is manifested as higher rolling moment at lower speeds. Slight leveling in the lift curves towards higher angles of attack was also observed in the free-hinge configuration as expected, since the fold angle increased with angle of attack. A similar trend was also present in the rolling moment as it was strongly influenced by the lift from the wing-tip. The hinge moments as shown in Figure 12 agree well with the fold angle measurements in Figure 11. In particular, a negative hinge moment at zero fold angle for the stiff-hinge configuration is complemented by a negative fold angle for the free-hinge configuration at the same angle of attack and continues to stay true when both the hinge moment and the fold angle became positive at 10° angle of attack. In Figure 13, the relationship between rolling moment and lift is linear for the stiff-hinge configuration and shows virtually no variations across different speeds as expected. The free-hinge configuration also exhibits linearity but with steeper gradient at lower speeds. Such behavior may be related back to the more negative fold angle at these speeds, causing higher lift at the wing-tip which adds to the rise in rolling moment.
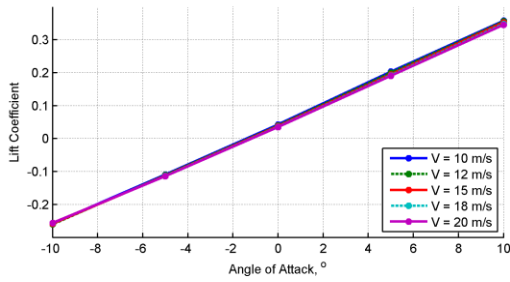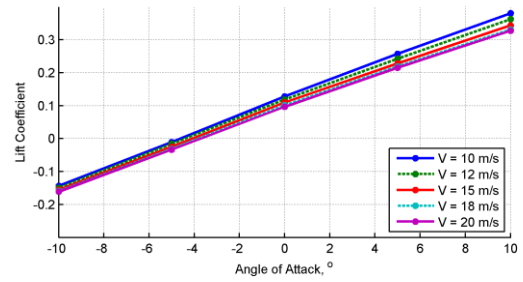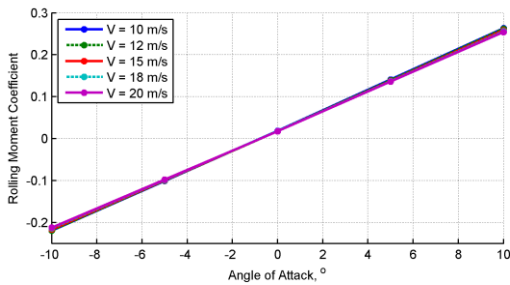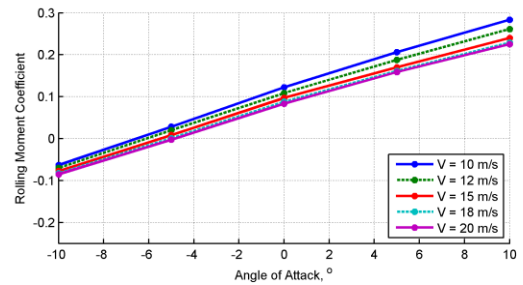
(a) Stiff-hinge configuration   (b) Free-hinge configuration

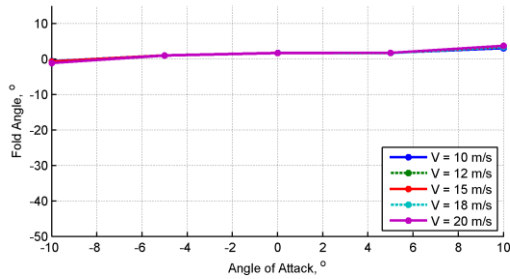**Figure 9. Variation of measured lift coefficient with angle of attack.**
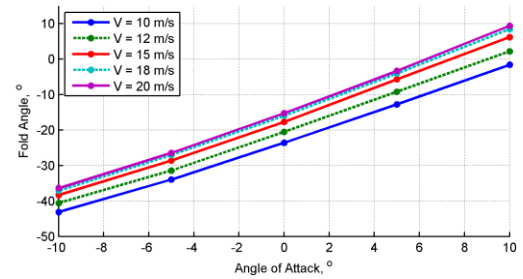

(a) Stiff-hinge configuration   (b) Free-hinge configuration

Figure 10. Variation of measured rolling moment coefficient with angle of attack.
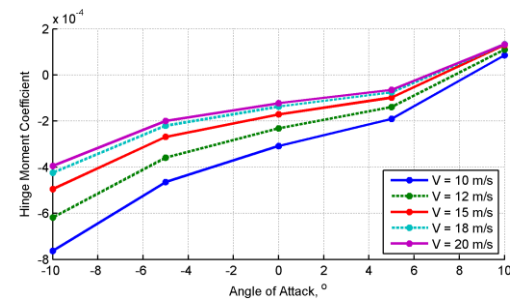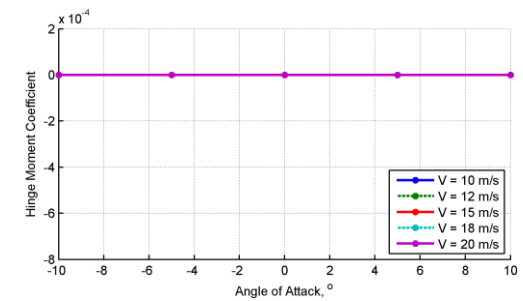

(a) Stiff-hinge configuration   (b) Free-hinge configuration

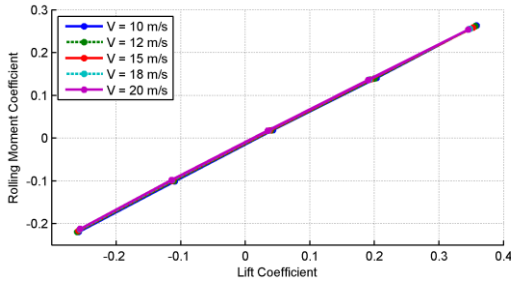**Figure 11. Variation of measured fold angle with angle of attack.**
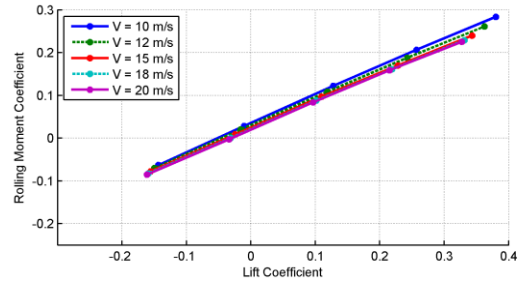

(a) Stiff-hinge configuration   (b) Free-hinge configuration

Figure 12. Variation of measured hinge moment coefficient with angle of attack.

6

American Institute of Aeronautics and Astronautics

(a) Stiff-hinge configuration　　　　　(b) Free-hinge configuration

Figure 13. Variation of measured rolling moment coefficient against measured lift coefficient.

B. Gust excitation

The stiff-hinge, sprung-hinge and free-hinge configuration were tested at wind speed of 20m/s, with angle of attack varying from -10° to 10° in increments of 5°. At each test point, the wind tunnel model was subjected to two types of gust excitation. A 'down-gust' excitation was initiated by pitching the gust vane downwards by 19.3° from its neutral position and released after the flow has stabilized at this perturbed state, while an 'up-gust' excitation was initiated by first pitching gust vane upwards by 8.7° and released in the same manner. These initial pitching deflection of the gust vane were made through displacing the counter-weight, which was part of the accompanying mass-spring system installation. This mass-spring system was underdamped and a few overshoots were observed through its motion, despite the inherent aerodynamic damping from the gust vane itself. At wind speed of 20m/s, this system had a frequency of approximately 4Hz.
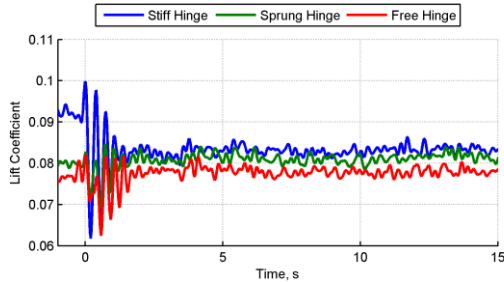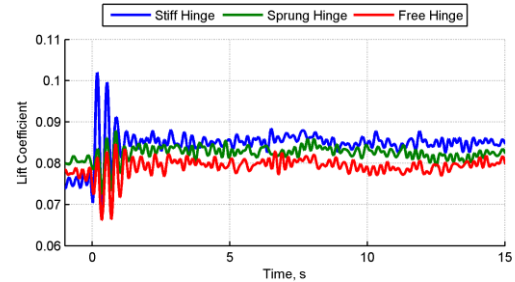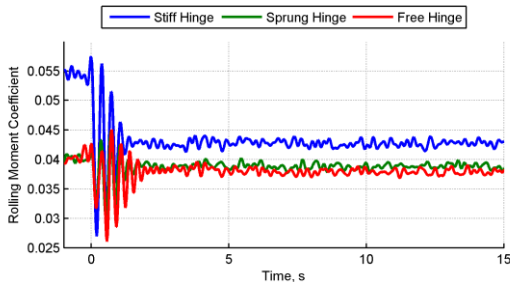

(a) Down-gust　　　　　(b) Up-gust

Figure 14. Lift coefficient response to gust at 10° angle of attack and wind speed of 20m/s.
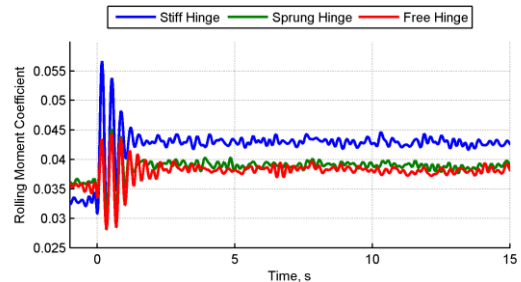
(a) Down-gust　　　　　(b) Up-gust

Figure 15. Rolling moment coefficient response to gust at 10° angle of attack and wind speed of 20m/s.

Figure 14 and Figure 15 show the typical response in lift and rolling moment during both gust excitations, while Figure 17 to Figure 19 (see Figure 20 for plot legend) show the upper and lower bound of the dynamic load envelope, as well as the perturbation in relation to their steady state in all test cases. These values have been

calculated using the definition shown in Figure 16, in which the perturbation is the change between the perturbed state and the steady state, while the upper and the lower bound are the difference between the maximum and the minimum from the steady state respectively. It is noted that a small difference across these steady states was present when compared with their corresponding steady aerodynamic test case, in which the gust vane was absent. However, the overall trends have not changed significantly.
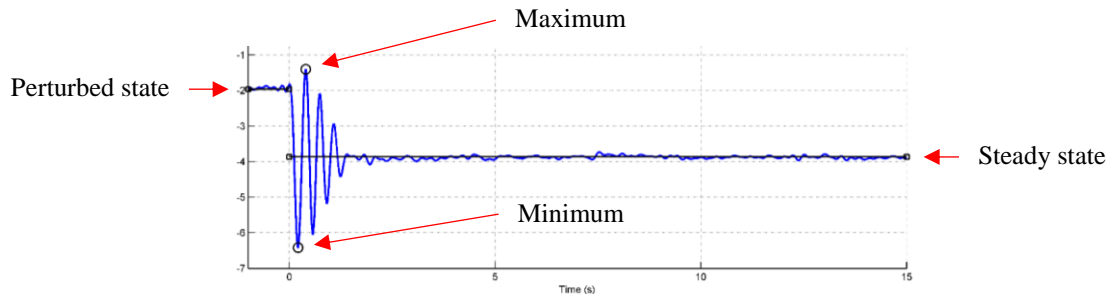

Figure 16. Terminology and their definitions in the context of the dynamic measurements.

From Figure 17, it can be seen that the changes in lift at the perturbed state for the sprung-hinge and free-hinge configuration were lower in magnitude than the stiff-hinge configuration. The allowable movement of the hinge in combination of the hinge angle allowed the wing-tip to offset some of the lift otherwise generated in a non-folding configuration. This offset in lift is shown to be beneficial because the changes in rolling moment, as illustrated in Figure 18, were also reduced in both hinge configurations. With lower loads in these perturbed states, it is unsurprising to also find the dynamic load envelope to be smaller for these hinge configurations. Given all these perturbations were caused by essentially the same change in upstream condition, it can be seen that a hinged wing-tip is less susceptible to additional loading caused by oncoming gusts.

For the sprung-hinge and free-hinge configuration, the change in lift in their respective perturbed state also appears to reduce at higher angles of attack, which coincided with the range of angles of attack that give fold angles around zero as shown in Figure 19. This finding suggests a hinged folding wing-tip configuration may receive less wing loading due to gust loads when the wing-tip is in level-trim in-flight. When examining the changes in rolling moments, as illustrated in Figure 18, a similar trend is observed. However, the reduction seen in the up-gust and down-gust cases were not the same and such asymmetric behavior is firstly attributed by the characteristics of the gust vane as seen through comparing against the stiff-hinge configuration. Secondly, the offset from the moment due to the weight of the wing-tip was also a contributing factor, because it could provide a restoring or an opposing moment towards the zero-fold angle position depending on the instantaneous orientation of the wing-tip itself. For the down-gust cases, the perturbed state always put the wing-tip in the negative fold angle region, as shown in Figure 19, which resulted in nose-up twist in the wing-tip. This shifted the lift distribution outboard to the wing-tip, adding to its rolling moment contribution. However, this effect was counteracted by the overall reduction in total lift, which ultimately resulted in the flatter variation observed. In comparison, the variation was more pronounced for the down-gust cases because their perturbed states varied from negative to positive fold angles.

The sprung-hinge configuration behaved similarly to the free-hinge configuration at most test points. As observed in Figure 18, the sprung-hinge configuration did not always produce a significantly reduced upper bound in rolling moment than the free-hinge configuration. However, trends from the sprung-hinge configuration show less variation across both gust cases, as for its trends in the lower bound of its dynamic load envelope. The overall rolling moment is comparable to the free-hinge configuration in the up-gust cases, but a significant advantage can be seen in the down-gust cases. The presence of the springs appears to reduce the extent to which folding of the wing-tip could occur, as indicated in Figure 19, but the reduction was not the same for both gust cases. Therefore, there is a strong suggestion that the weight of the wing-tip and its associated moment has a substantial effect on the overall performance of the wing-tip device. For positive angles of attack, the effect from the springs alone was more noticeable in the upper bounds than in the lower bounds of the fold angle. Upon considering the rolling moments as shown in Figure 18, the free-hinge configuration in fact performed marginally better the sprung-hinge configuration at this range of angles of attack. However, it should be noted that the sprung-hinge configuration developed a smaller dynamic load envelope during the down-gust events at high angles of attack, as the lower bounds were closer in magnitude to their corresponding steady state rolling moment.
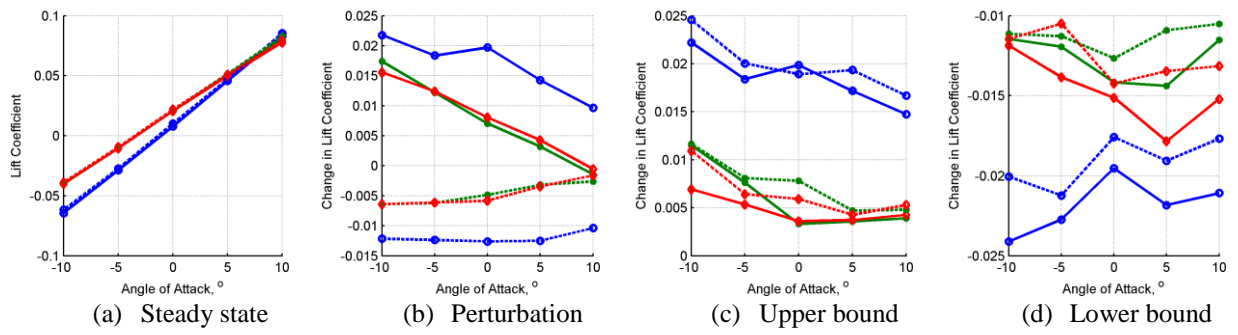
American Institute of Aeronautics and Astronautics

Figure 17 Lift coefficient in response to gust at various angles of attack.
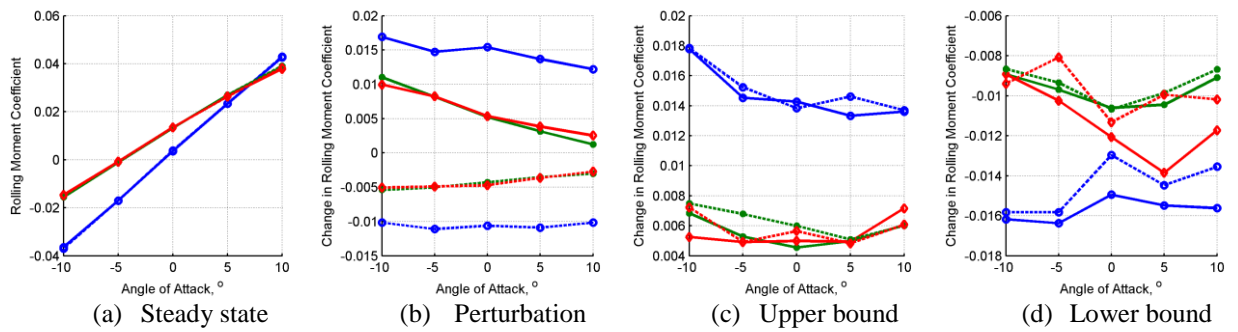

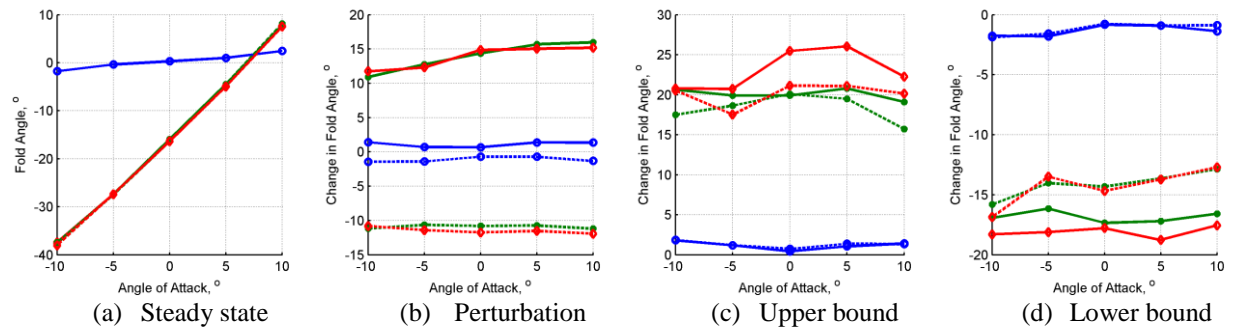**Figure 18. Rolling moment coefficient in response to gust at various angles of attack.**

Figure 19. Fold angle in response to gust at various angles of attack.

Figure 20. Legend for Figure 17 to Figure 19.

IV. Conclusions

A series of low-speed wind tunnel tests have been carried out to investigate the aerodynamic performance a folding wing-tip prototype with a 30° hinge angle. The tests examined the behavior of the wing-tip and the overall loading with varying hinge stiffness under steady aerodynamic conditions as well as when responding to gust excitations.

In the steady aerodynamic tests, a free-hinge configuration, of no added torsional stiffness at the folding hinge, was found to be statically aerodynamically stable. The lift-curve from this free-hinge configuration was less steep than the stiff-hinge configuration and became even shallower at higher angles of attack due to the more positive fold angle. Reducing speed produced higher lift coefficients because the fold angle became more negative, causing additional positive effective twist in the wing-tip thus higher overall lift. The rolling moments followed the same trend since these effects in lift impacted the overall rolling moment in a similar manner.

From the gust excitation tests, both the free-hinge configuration and the sprung-hinge configuration of intermediate added hinge stiffness, performed significantly better than the stiff-hinge configuration in reducing the peak increase in rolling moment in both upward and downward gust excitations, and thus provided gust loads alleviation capability. In particular, the free-hinge configuration appeared to marginally outperform the sprung-hinge configuration in the upward gust test cases, but less effective in the downward gust test cases. This finding suggests the combination of wing-tip weight and hinge stiffness has a significant effect on its performance as predicted by the previous simulation studies[14]. For the sprung-hinge configuration, it was also observed that the dynamic load envelope developed during these gust events were smaller.

Acknowledgments

References

[1]Livne E., Weisshaar T.A., Aeroelasticity of nonconventional airplane configurations-past and future, Journal of Aircraft, 40(6), pp.1047-1065, 2003.

[2]Friswell M.I., The prospects for morphing aircraft, in Smart Structures and Materials (SMART09), IV ECCOMAS Thematic Conference (pp. 175-188), 2009.

[3]Sofla A.Y.N., Meguid S.A., Tan K.T., Yeo W.K., Shape morphing of aircraft wing: status and challenges, Materials & Design, 1(3), pp.1284-1292, 2010.

[4]Barbarino S., Bilgen O., Ajaj R.M., Friswell M.I., Inman D.J., A review of morphing aircraft. Journal of Intelligent Material Systems and Structures, 22(9), pp.823-877, 2011.

[5]Ajaj R.M., Beaverstock C.S., Friswell M.I., Morphing aircraft: the need for a new design philosophy, Aerospace Science and Technology, 49, pp.154-166, 2016.

[6]Sun J., Guan Q., Liu Y., Leng J., Morphing aircraft based on smart materials and structures: A state-of-the-art review, Journal of Intelligent Material Systems and Structures, p.1045389X16629569, 2016.

[7]Cooper J.E., Chekkal I., Cheung R.C.M., Wales C., Allen N.J., Lawson S., Peace A.J., Cook R., Standen P., Hancock S.D., Carossa G.M., Design of a Morphing Wingtip, Journal of Aircraft, 52(5), pp.1394-1403, 2015.

[8]Smith M.H., Renzelmann M.E., Marx A.D., The Boeing Company, 1995. Folding wingtip system. U.S. Patent 5,381,986.

[9]Miller S., Vio G.A., Cooper J.E., Sensburg O., Optimisation of a scaled sensorcraft model with passive gust alleviation, in Proceedings of the 12th AIAA/ISSMO Multidisciplinary Analysis and Optimization Conference, MAO, Victoria, BC, Canada (Vol. 1012), 2008.

[10]Miller S., Vio G.A., Cooper J.E., Development of an Adaptive Wing Tip Device, 50th AIAA/ASME/ASCE/AHS/ASC Structures, Structural Dynamics, and Materials Conference, 2009.

[11]Guo S., Fu Q., Sensburg O.K., Optimal design of a passive gust alleviation device for a flying wing aircraft, in Proceedings of the 12th AIAA ATIO/14th AIAA/ISSMO MAO Conference, Session MAO-25, Indianapolis, IN, USA (Vol. 1719), 2012.

[12]Guo S., Los Monteros D., Espinosa J., Liu Y., Gust Alleviation of a Large Aircraft with a Passive Twist Wingtip, Aerospace, 2(2), pp.135-154, 2015.

[13]Ricci S., Castellani M., Romanelli G., Multi-fidelity design of aeroelastic wing tip devices, Proceedings of the Institution of Mechanical Engineers, Part G: Journal of Aerospace Engineering, p.0954410012459603, 2012.

[14]Castrichini A., Hodigere Siddaramaiah. V., Calderon. D.E., Cooper J.E., Wilson T. & Lemmens Y., "Preliminary Investigation of Use of Flexible Folding Wing-Tips for Static and Dynamic Loads Alleviation", Aeronautical Journal -New Series- · November 2016, DOI: 10.1017/aer.2016.108.

[15]Gatto A., Mattioni F. and Friswell M. I., "Experimental Investigation of Bistable Winglets to Enhance Aircraft Wing Lift Takeoff Capability", Journal of Aircraft, Vol. 46, No. 2 (2009), pp. 647-655.

[16]Arrieta A. F., Bilgen O., Friswell M. I., Hagedorn P., "Dynamic control for morphing of bi-stable composites", Journal of Intelligent Material Systems and Structures, 24(3) 266–273.

[17]Castrichini A., Hodigere Siddaramaiah. V., Calderon. D.E., Cooper J.E., Wilson T. & Lemmens Y., "Nonlinear Folding Wing-Tips for Gust Loads Alleviation", Journal of Aircraft · February 2016, DOI: 10.2514/1.C033474.

[18]Castrichini A., Cooper J.E., Wilson T., A. Carrella & Lemmens Y., "Nonlinear Negative Stiffness Wing-Tip Spring Device for Gust Loads Alleviation", in Journal of Aircraft · November 2016, DOI: 10.2514/1.C033887.

[19]http://www.amti.uk.com/, retrieved December 02, 2016

[20]http://www.rls.si/, retrieved December 02, 2016

[21]http://www.rdpe.com/uk/men-load.htm, retrieved December 02, 2016

[22]http://www.ni.com/en-gb.html, retrieved December 02, 2016